Ab initio calculations of the electronic structure and linear optical properties, including self-energy effects, for paraelectric SbSI

2007 J. Phys.: Condens. Matter 19 116207

(http://iopscience.iop.org/0953-8984/19/11/116207)

IOP PUBLISHING JOURNAL OF PHYSICS: CONDENSED MATTER

J. Phys.: Condens. Matter **19** (2007) 116207 (10pp) doi:10.1088/0953-8984/19/11/116207

Ab initio calculations of the electronic structure and linear optical properties, including self-energy effects, for paraelectric SbSI

Harun Akkus and Amirullah M Mamedov

Department of Physics, Cukurova University, 01330 Adana, Turkey

E-mail: hakkus@cu.edu.tr and mamedov@cu.edu.tr

Received 3 September 2006, in final form 31 January 2007
Published 5 March 2007
Online at stacks.iop.org/JPhysCM/19/116207

Abstract

The electronic energy band structure and linear optical properties of the ferroelectric semiconductor SbSI in the paraelectric phase are calculated by an *ab initio* pseudopotential method using density functional theory in the local density approximation. The calculated electronic band structure shows that SbSI has an indirect band gap of 1.45 eV and that the smallest direct gap is at the S point of the Brillouin zone (1.56 eV). The total density of states has been analysed. The linear energy dependent dielectric functions and some optical constants such as the absorption coefficient, extinction coefficient, refractive index, energy-loss function, reflectivity and optical conductivity, including self-energy effects, are calculated. The effective number of valence electrons and the effective optical dielectric constant are also calculated.

1. Introduction

Antimony sulfo-iodide (SbSI), as the most well known member of the group of $A^{V}B^{VI}C^{VII}$ (A = Sb, Bi, As; B = S, Se, O; C = I, Br, Cl) compounds, has been attractive for its fundamental research interest and prospective applications in the fields of ferroelectricity, microelectronics and optoelectronics, as microcapacitors, optical valves, and so on. According to Dönges [1] the crystal structure of SbSI is orthorhombic. The point group of SbSI is *mmm* (space group D_{2h}^{16}) in the paraelectric phase above the Curie point and *mm*2 (space group C_{2v}^{9}) in the ferroelectric phase below the Curie point. Nitsche and Merz [2] have reported that SbSI is a photoconductor with a maximum sensitivity at 6300–6400 Å. Fatuzzo *et al* [3] have reported that SbSI is ferroelectric and its Curie point is 22 °C. The crystal structure of SbSI is shown figure 1. This crystal has four SbSI molecules (12 atoms) in a unit cell. Each molecule of SbSI extends in a chain-like fashion along the *c*-axis which is also the polarization axis. The atomic positions in the unit cell are given in table 1.

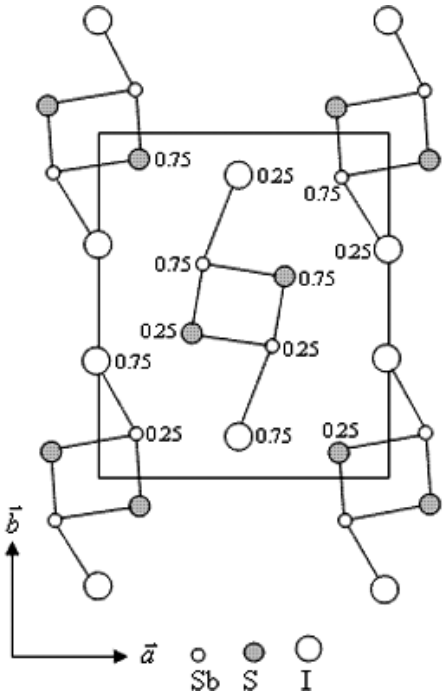

Figure 1. Schematic projection of the SbSI molecules on the xy-plane in the paraelectric phase.

Table 1. Atomic positions of each of the atoms in the unit cell of paraelectric SbSI [4].

	Para. (35 °C)		
α	X_α	Y_α	Z_α
Sb	0.119	0.124	0.250
S	0.840	0.050	0.250
I	0.508	0.828	0.250

The band structure of SbSI has been investigated using semi-empirical [4], empirical [5], and *ab initio* [6] pseudopotential methods. The band structure of SbSI was calculated for the paraelectric and ferroelectric phases [4, 5] and also for the paraelectric phase [6]. The optical properties of SbSI have been widely studied [4, 7–13] since the 1960s due to its semiconducting and ferroelectric properties; however, there is no *ab initio* calculation of the optical properties of SbSI in the literature.

In the present work, we have investigated and calculated the electronic band structure and the linear optical properties of the paraelectric SbSI crystal using a pseudopotential method based on the density functional theory (DFT) in the local density approximation (LDA) [14]. Firstly, the band structure and the total density of states (DOS) of paraelectric SbSI were calculated. Then the linear frequency dependent optical dielectric functions including the self-energy effects and some optical functions, the absorption coefficient, $\alpha(\omega)$, extinction coefficient, $k(\omega)$, refractive index, $n(\omega)$, energy-loss spectrum, $L(\omega)$, reflectivity, $R(\omega)$, optical conductivity, $\sigma(\omega)$, effective number of valence electrons per unit cell, $N_{\text{eff}}(\omega)$, and effective optical dielectric function, $\varepsilon_{\text{eff}}(\omega)$, were calculated. In the calculations of the optical response,

according to the band structure calculated by us, we have chosen a photon energy range of 0–16 eV and seen that a 0–8 eV photon energy range is sufficient for most optical functions.

2. Computational details

The self-consistent norm-conserving pseudopotentials were generated by using FHI98PP code [15] with the Troullier–Martins scheme [16]. Plane waves were used as the basis set for the electronic wavefunctions. In order to solve the Kohn–Sham equations [14], the conjugate gradient minimization method [17] was employed in the ABINIT code [18]. The exchange–correlation effects were taken into account within the Perdew–Wang (PW92) scheme [19] in the LDA in the pseudopotential, the band structure and optical response calculations. For Sb and I atoms 5s and 5p electrons, and for S atom 3s and 3p electrons were considered as the true valence.

All the calculations involve a 12-atom orthorhombic unit cell. Good convergence for the bulk total energy calculation has been achieved with the choice of cut-off energies at 12 Hartree using a $4 \times 4 \times 4$ Monkhorst–Pack [20] mesh grid. We have found that in the band structure calculations 64 **k** points are enough for obtaining good results for SbSI. In the optical properties calculations, however, the irreducible Brillouin zone (BZ) has been sampled with a $24 \times 24 \times 24$ Monkhorst–Pack grid for SbSI.

It is well known that the effect of the electric field vector, $\mathbf{E}(\omega)$, of the incoming light is to polarize the material. At the level of linear response this polarization can be calculated using the following relation [21]:

$$P^i(\omega) = \chi^{(1)}_{ij}(-\omega, \omega) \cdot E^j(\omega), \tag{1}$$

where $\chi^{(1)}_{ij}$ is the linear optical susceptibility tensor and it is given by [21, 22]

$$\chi^{(1)}_{ij}(-\omega, \omega) = \frac{e^2}{\hbar\Omega} \sum_{nm\vec{k}} f_{nm}(\vec{k}) \frac{r^i_{nm}(\vec{k})\, r^j_{mn}(\vec{k})}{\omega_{mn}(\vec{k}) - \omega} = \frac{\varepsilon_{ij}(\omega) - \delta_{ij}}{4\pi} \tag{2}$$

where n, m denote energy bands, $f_{mn}(\vec{k}) \equiv f_m(\vec{k}) - f_n(\vec{k})$ is the Fermi occupation factor, Ω is the normalization volume. $\omega_{mn}(\vec{k}) \equiv \omega_m(\vec{k}) - \omega_n(\vec{k})$ are the frequency differences, $\hbar\omega_n(\vec{k})$ is the energy of band n at wavevector **k**. The $\vec{r}_{nm}$ are the matrix elements of the position operator and are given by [22]

$$\begin{aligned} r^i_{nm}(\vec{k}) &= \frac{v^i_{nm}(\vec{k})}{\mathrm{i}\omega_{nm}}; \qquad \omega_n \neq \omega_m \\ r^i_{nm}(\vec{k}) &= 0; \qquad \omega_n = \omega_m \end{aligned} \tag{3}$$

where $v^i_{nm}(\vec{k}) = m^{-1} p^i_{nm}(\vec{k})$, m is the free electron mass, and $\vec{p}_{nm}$ is the momentum matrix element.

As can be seen from equation (2), the dielectric function $\varepsilon_{ij}(\omega) = 1 + 4\pi\chi^{(1)}_{ij}(-\omega, \omega)$ and the imaginary part of $\varepsilon_{ij}(\omega)$, $\varepsilon^{ij}_2(\omega)$, is given by

$$\varepsilon^{ij}_2(\omega) = \frac{e^2}{\hbar\pi} \sum_{nm} \int \mathrm{d}\vec{k}\, f_{nm}(\vec{k}) \frac{v^i_{nm}(\vec{k}) v^j_{mn}(\vec{k})}{\omega^2_{mn}} \delta(\omega - \omega_{mn}(\vec{k})). \tag{4}$$

The real part of $\varepsilon_{ij}(\omega)$, $\varepsilon^{ij}_1(\omega)$, can be obtained by using the Kramers–Kronig transformation:

$$\varepsilon^{ij}_1(\omega) - 1 = \frac{2}{\pi} \wp \int_0^\infty \frac{\omega' \varepsilon^{ij}_2(\omega')}{\omega'^2 - \omega^2} \mathrm{d}\omega'. \tag{5}$$

Because the Kohn–Sham equations determine the ground state properties, the unoccupied conduction bands as calculated have no physical significance. If they are used as single-particle states in a calculation of optical properties for semiconductors, a band gap problem comes into existence: the absorption starts at too low an energy [21]. The many-body effects must be included in calculations of response. In order to take into account self-energy effects, in the present work, we used the 'scissors approximation' [23].

Within the scissors approximation the Hamiltonian from which response functions are calculated is given by

$$\tilde{H} = H + V_s \tag{6}$$

where

$$H = \frac{p^2}{2m} + V(\vec{r}) - e\,\vec{r}\cdot\vec{E} \tag{7}$$

and

$$V_s = \Delta \sum_{c\vec{k}} |c\vec{k}\rangle\,\langle c\vec{k}| \tag{8}$$

is the scissors operator [21]. In this expression the sum is over all **k** and conduction bands c, Δ is the constant energy shift related to the correction of the band gap, and $|c\vec{k}\rangle$ denotes single-particle eigenstates of the unperturbed Hamiltonian. In the framework of the scissors approximation, equation (2) can be rewritten as follows:

$$\chi^{(1)}_{ij}(-\omega,\omega) = \frac{e^2}{\hbar\Omega}\sum_{nm\vec{k}} f_{nm}(\vec{k})\frac{r^i_{nm}(\vec{k})\,r^j_{mn}(\vec{k})}{\omega_{mn}(\vec{k}) + \frac{\Delta}{\hbar}(\delta_{mc}-\delta_{nc}) - \omega}. \tag{9}$$

The difference between equations (2) and (9) is only the modification of the frequencies ω_{mn}, $\omega_{mn} \to \frac{\Delta}{\hbar}(\delta_{mc}-\delta_{nc})$. In the present work, Δ, the scissor shift to make the theoretical band gap match the experimental one, is $\Delta = 0.66$ eV.

Expressions for the absorption coefficient, $\alpha(\omega)$, extinction coefficient, $k(\omega)$, refractive index, $n(\omega)$, energy-loss spectrum, $L(\omega)$, reflectivity, $R(\omega)$, and optical conductivity, $\sigma(\omega)$, are given as follows, respectively:

$$\begin{aligned}
\alpha_{ii}(\omega) &= \frac{2\omega}{c}k_{ii}(\omega),\\
k_{ii}(\omega) &= \left\{\frac{1}{2}\left[\left[(\operatorname{Re}\varepsilon_{ii}(\omega))^2 + (\operatorname{Im}\varepsilon_{ii}(\omega))^2\right]^{1/2} - \operatorname{Re}\varepsilon_{ii}(\omega)\right]\right\}^{1/2},\\
n_{ii}(\omega) &= \left\{\frac{1}{2}\left[\left[(\operatorname{Re}\varepsilon_{ii}(\omega))^2 + (\operatorname{Im}\varepsilon_{ii}(\omega))^2\right]^{1/2} + \operatorname{Re}\varepsilon_{ii}(\omega)\right]\right\}^{1/2},\\
L_{ij}(\omega) &= -\operatorname{Im}\varepsilon^{-1}_{ij}(\omega),\\
R_{ii}(\omega) &= \frac{(n_{ii}-1)^2 + k^2_{ii}}{(n_{ii}+1)^2 + k^2_{ii}}\\
\operatorname{Re}\sigma_{ij}(\omega) &= \frac{\omega}{4\pi}\operatorname{Im}\varepsilon_{ij}(\omega).
\end{aligned} \tag{10}$$

The known sum rules [24] can be used to determine some quantitative parameters, particularly the effective number of the valence electrons per unit cell N_{eff}, as well as the effective optical dielectric constant $\varepsilon_{\mathrm{eff}}$, which make a contribution to the optical constants of a crystal at the energy E_0. One can obtain an estimate of the distribution of oscillator strengths for both intraband and interband transitions by computing the $N_{\mathrm{eff}}(E_0)$ defined according to

$$N_{\mathrm{eff}}(E) = \frac{2m\varepsilon_0}{\pi\hbar^2 e^2 N_{\mathrm{a}}}\int_0^{E_0} \varepsilon_2(E)E\,\mathrm{d}E, \tag{11}$$

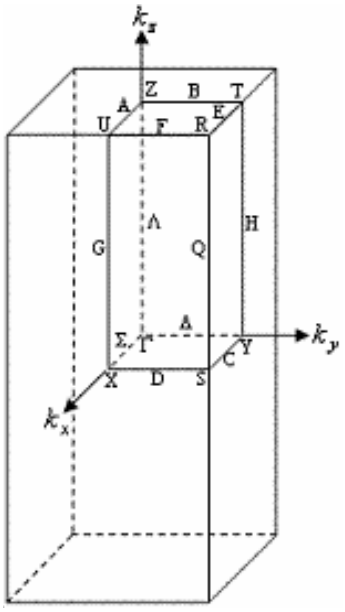

Figure 2. The first Brillouin zone of the SbSI crystal.

where N_a is the density of atoms in a crystal, e and m are the charge and mass of the electron, respectively and $N_{eff}(E_0)$ is the effective number of electrons contributing to optical transitions below an energy of E_0.

Further information on the role of the core and semi-core bands may be obtained by computing the contribution which the various bands make to the static dielectric constant, ε_0. According to the Kramers–Kronig relations, one has

$$\varepsilon_0(E) - 1 = \frac{2}{\pi} \int_0^\infty \varepsilon_2(E) E^{-1} \, \mathrm{d}E. \tag{12}$$

One can therefore define an 'effective' dielectric constant, which represents a different mean of the interband transitions from that represented by the sum rule, equation (12), according to the relation

$$\varepsilon_{eff}(E) - 1 = \frac{2}{\pi} \int_0^{E_0} \varepsilon_2(E) E^{-1} \, \mathrm{d}E. \tag{13}$$

The physical meaning of ε_{eff} is quite clear: ε_{eff} is the effective optical dielectric constant governed by the interband transitions in the energy range from zero to E_0, i.e. by the polarization of the electron shells.

3. Results and discussion

The notation for the high symmetry points between which we have drawn the band structure corresponds to that chosen in [25] and the outcome is shown in figure 2. The calculated band structure of SbSI in the paraelectric phase is presented in figure 3. We have observed the presence of well separated groups of bands in the paraelectric phase. As previously discussed [8, 26], the chemical bonding in SbSI has a mixed covalent–ionic character. According to [26] the bond between antimony and sulfur atoms in the chain is covalent while the iodine ion is in an ionic bond with a covalently bound bridge $(SbS)^+$.

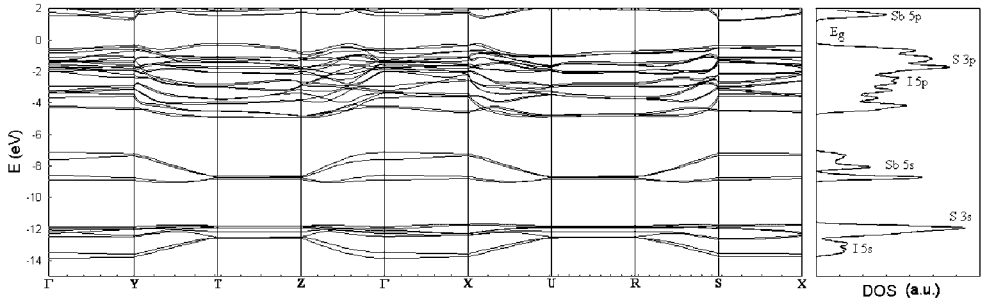

Figure 3. Electronic band structure and the corresponding total density of states of paraelectric SbSI (the atomic positions at 35 °C [4] are used in the calculations).

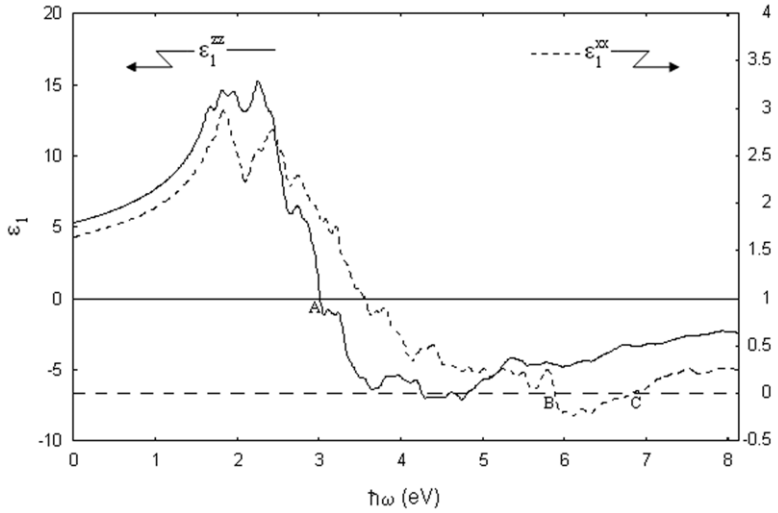

Figure 4. Real parts of the xx- and zz-components of the linear dielectric tensor in paraelectric SbSI.

In figure 3, shown in the rightmost panel is the normalized total density of states (DOS) for the SbSI crystal. The valence band is composed of 5s and 5p orbitals of the I atom, 3s and 3p orbitals of the S atom, and 5s orbitals of the Sb atom, while the conduction band consists of 5p orbitals of the Sb atom.

As can be seen in figure 3, the SbSI crystal has an indirect forbidden gap in the paraelectric phase. The minimum of the conduction band is located at the S point of the BZ, 1.24 eV. The maximum of the valence band is located at the T point of the BZ, −0.21 eV. The value of the forbidden gap is 1.45 eV. Our results coincide with the data given in [4–8, 26]. The indirect gap, E_g, increases from 1.45 eV (T → S) to 2.91 eV (Z → U). The direct band gap, E_g, increases from 1.56 eV (at the S point) to 3.11 eV (at the U point).

Because of the orthorhombic crystal symmetry, the linear dielectric tensor of the SbSI crystal has three independent components which are diagonal elements of the linear dielectric tensor [27]. The calculated real parts of the xx- and zz-components of the linear frequency dependent dielectric function are presented in figure 4. ε_1^{xx} equals zero at about 3 eV (at the A point in figure 4) and ε_1^{zz} equals zero at about 5.9 eV and 6.9 eV (at the B and C points in

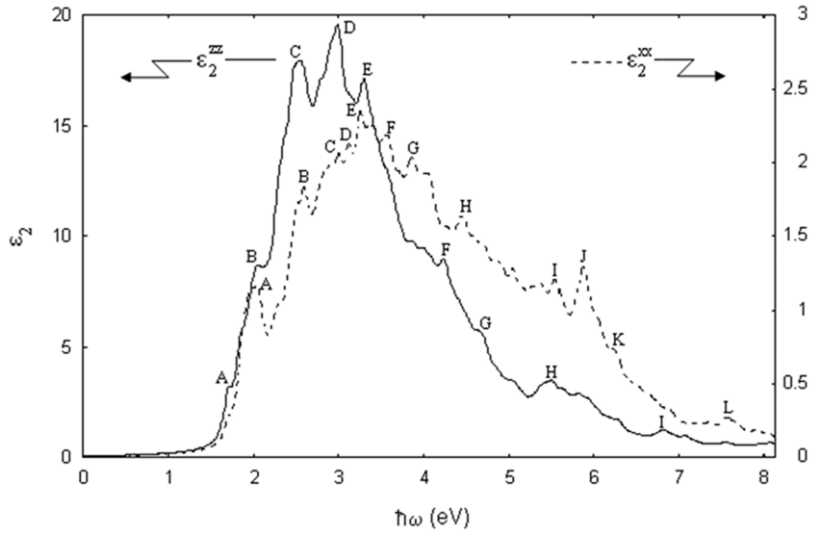

Figure 5. Imaginary parts of the xx-and zz-components of the linear dielectric tensor in paraelectric SbSI.

Table 2. Comparative characteristics of linear optical functions of paraelectric SbSI crystal (*ab initio* calculation).

	Peaks (eV)											
ε_2	A	B	C	D	E	F	G	H	I	J	K	L
xx	1.98	2.56	3.00	3.13	3.25	3.56	3.84	4.48	5.54	5.85	6.24	7.58
zz	1.70	2.05	2.52	2.98	3.30	4.24	4.65	5.48	6.80	—	—	—

figure 4). The imaginary parts of the linear frequency dependent dielectric function along the x- and z-directions are illustrated in figure 5. The values of the ε_2^{xx} and ε_2^{zz} peaks shown in figure 5 are summarized in table 2. The peaks correspond to the transitions from the valence to the conduction band (see figure 5).

The calculated energy-loss functions, $-\operatorname{Im}\varepsilon^{-1}$, are presented in figure 6. In this figure, L_{xx} and L_{zz} correspond to the energy-loss functions along the x- and z-directions, respectively. The function $-\operatorname{Im}\varepsilon^{-1}$ describes the energy loss of fast electrons traversing the material. The sharp maxima in the energy-loss function are associated with the existence of plasma oscillations [28]. The curve of L_{xx} in figure 6 has a maximum near 6.9 eV and this value coincides with the C point in figure 4. The curve of L_{zz} in figure 6 has a maximum near 15.5 eV.

The calculated refractive indices and extinction coefficients along the x- and z-axes are presented in figure 7. As can be seen from figures 7(a) and (b), normal dispersion exists in the 0–1.5 eV energy range. This is consistent with results for ε_2 in figure 5. The photon energy range between 1.5 and 6 eV corresponds to an absorption region. The calculated absorption coefficients and reflectivities along the x- and z-axes are shown in figure 8. In accordance with the optical functions calculated and presented above, the absorption starts near 1.5 eV (see figure 8(a)). In figure 8(b), in addition to the calculated reflectivities, along the x- and z-axes, experimental data [13] are reproduced.

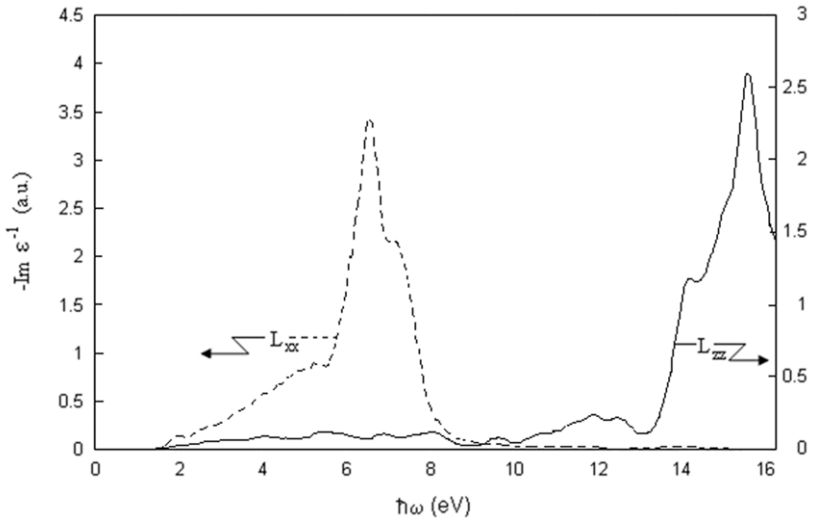

Figure 6. Energy-loss functions along the x- and z-axes (polar axis c).

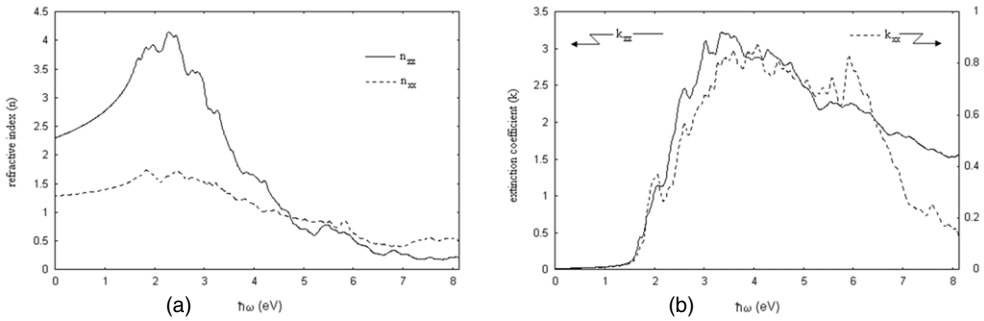

Figure 7. Refractive indices (a) and extinction coefficients (b) along the x- and z-axes (polar axis c).

The calculated optical conductivities are illustrated in figure 9(a). The effective number of valence electrons and the effective dielectric constant are given in figure 9(b). The maximum values of the optical conductivity appear at about 0.34 μm and 0.4 μm in the directions of the x- and z-axes, respectively (see figure 9(a)). The effective number of valence electrons per unit cell, N_{eff}, contributing in the interband transitions, reaches a saturation value at about 9 eV. This shows that the deep-lying valence orbitals do not participate in the interband transitions (see figure 9(b)). The effective optical dielectric constant, ε_{eff}, shown in figure 9(b) reaches a saturation value at about 7 eV. The photon energy dependence of ε_{eff} obtained by us for SbSI is a curve which can be separated into two regions. The first is characterized by a rapid rise and it extends up to 5.0 eV. In the second region the value of ε_{eff} rises more smoothly and slowly and tends to saturation at the energies 7 eV. The contribution to the static dielectric constant made by optical transitions at photon energies $E > E_0$ can be determined by comparing the maximum value of ε_{eff} with the square of the refractive index n^2 measured in the transparency range [8]. The difference $\delta\varepsilon = n^2 - \varepsilon_{\text{eff}} \neq 0$ ($\delta\varepsilon \approx 1.8$) shows the need to allow for the

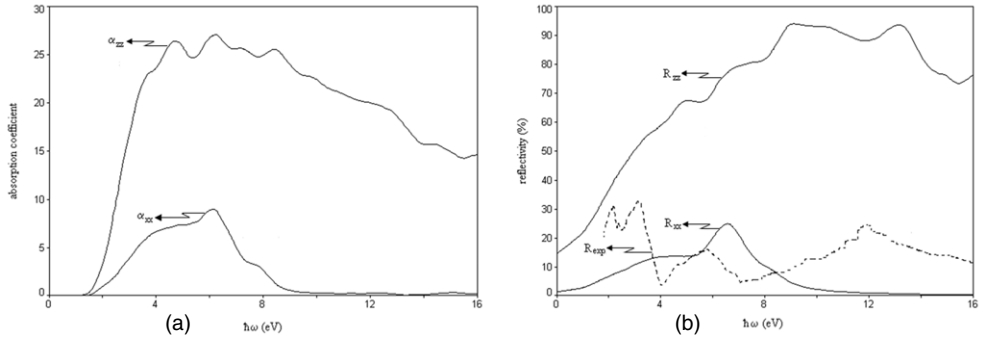

Figure 8. Absorption coefficients (a) and reflectivities (b) along the x- and z-axes (polar axis c). (R_{exp} was measured in the plane perpendicular to the z-axis and the polarization for synchrotron radiation has the geometry $\mathbf{E} \perp \mathbf{z}$ [13].)

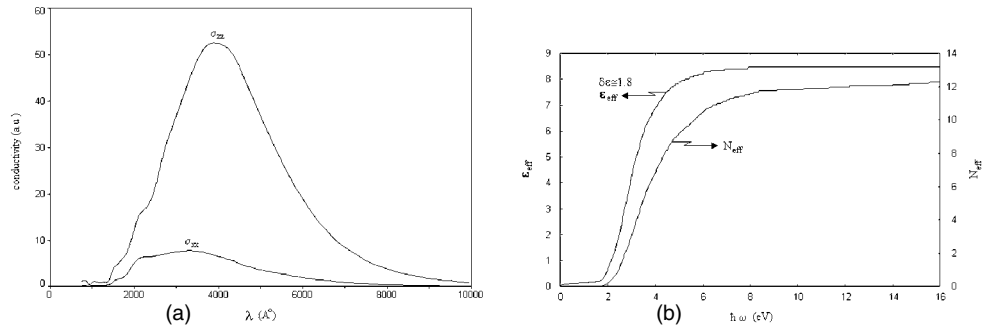

Figure 9. Optical conductivities along the x- and z-axes (polar axis c) (a) and the effective number of valence electrons and effective optical dielectric constant (b).

polarizability of deep-lying levels. The difference indicates that a large contribution to the static dielectric constant is made by interband transitions with $E > E_0$. This means that the greatest contribution to ε_{eff} arises from interband transitions between 1.5 and 7 eV.

4. Conclusions

In the present work, we have made a detailed investigation of the electronic structure and linear optical properties of paraelectric SbSI using the *ab initio* pseudopotential method. Our objective was to apply the density functional methods to the non-polar phase of the ferroelectric semiconductor SbSI. We have seen that the paraelectric SbSI crystal has an indirect forbidden gap, and has the smallest direct gap at the S point of the BZ. The total DOS calculation shows that the valence band is composed of 5s and 5p orbitals of the I atom, 3s and 3p orbitals of the S atom and 5s orbitals of the Sb atom while the conduction band consists of 5p orbitals of the Sb atom. We have examined photon energy dependent dielectric functions as well as related quantities such as absorption coefficients, extinction coefficients, refractive indices, energy-loss functions, reflectivities and optical conductivities along the x- and z-axes. Lastly, we have calculated the effective number of valence electrons per unit cell participating in the interband transitions and the effective optical dielectric function.

References

[1] Dönges E Z 1950 *Anorg. Chem.* **263** 112
Dönges E Z 1951 *Anorg. Chem.* **265** 56
[2] Nitsche R and Merz W J 1960 *J. Phys. Chem. Solids* **13** 154
[3] Fattuzo E, Harbeke G, Merz W J, Nitsche R, Roetschi H and Ruppel W 1962 *Phys. Rev.* **127** 2036
[4] Nakao K and Balkanski M 1973 *Phys. Rev.* B **8** 5759
[5] Audzijonis A, Zaltauskas R, Audzijoniene L, Vinokurova I V, Farberovich O V and Sadzius R 1998 *Ferroelectrics* **211** 111
[6] Bercha D M, Rushchanskii K Z, Sznajder M, Matkovskii A and Potera P 2002 *Phys. Rev.* B **66** 195203
[7] Masuda Y, Sakata K, Hasegawa S, Ohara G, Wada M and Nishizawa M 1969 *Japan. J. Appl. Phys.* **8** 692
[8] Gerzanich E I, Lyakhovitskaya V A, Fridkin V M and Popovkin B A 1982 *Current Topics in Materials Science. SbSI and Other Ferroelectric* $A^{V}B^{VI}C^{VII}$ *Materials* (Amsterdam: North-Holland)
[9] Toyoda K 1986 *Ferroelectrics* **69** 201
[10] Cross L E, Bhalla A, Ainger F and Damjakovic D 1991 *US Patent Specification* 4994. 672
[11] Mamedov A M 1977 *Sov. Phys.—Solid State* **19** 845 (in Russian)
[12] Surthi S, Kotru S and Pandey R 2003 *J. Mater. Sci. Lett.* **22** 591
[13] Mamedov A M, Aliev A O, Kasumov B M and Efendiev S M 1988 *Ferroelectrics* **83** 157
[14] Kohn W and Sham L J 1965 *Phys. Rev.* **140** A1133
[15] Fuchs M and Scheffler M 1999 *Comput. Phys. Commun.* **119** 67
[16] Troullier N and and Martins J L 1990 *Phys. Rev.* B **43** 1993
[17] Payne M C, Teter M P, Allan D C, Arias T A and Joannopoulos J D 1992 *Rev. Mod. Phys.* **64** 1045
[18] Gonze X, Beuken J M, Caracas R, Detraux F, Fuchs M, Rignanese G M, Sindic L, Verstrate M, Zerah G, Jollet F, Torrent M, Roy A, Mikami M, Ghosez P, Raty J Y and Allan D C 2002 *Comput. Mater. Sci.* **25** 478 URL http://www.abinit.org
[19] Perdew J P and Wang Y 1992 *Phys. Rev.* B **45** 13244
[20] Monkhorst H J and Pack J D 1976 *Phys. Rev.* B **13** 5188
[21] Hughes J L P and Sipe J E 1996 *Phys. Rev.* B **53** 10751
[22] Sharma S and Ambrosch-Draxl C 2004 *Phys. Scr.* T **109** 128
[23] Levine Z H and Allan D C 1989 *Phys. Rev. Lett.* **63** 1719
[24] Philipp H R and Ehrenreich H 1963 *Phys. Rev.* **129** 1550
[25] Kovalev O V 1993 *Representations of the Crystallographic Space Groups. Irreducible Representations, Induced Representations and Corepresentations* ed H T Stokes and D M Hatch (Amsterdam: Gordon and Breach)
[26] Alward J F, Fong C Y, El-Batanouny M and Wooten F 1978 *Solid State Commun.* **25** 307
[27] Nye J F 1957 *Physical Properties of Crystals* (Oxford: Clarendon)
[28] Marton L 1956 *Rev. Mod. Phys.* **28** 172